Capítulo 1 PM_1 en el aire exterior: fuentes, contenido de especies iónicas y propiedades alcalinas en el Área Metropolitana de Guadalajara, Jalisco-México

Chapter 1 PM_1 in outdoor air: sources, ion species content and alkaline properties in the Guadalajara Metropolitan Area, Jalisco-Mexico

OJEDA-CASTILLO, Valeria†[1.2], SÁNCHEZ-TORRES, Perla Berenice[1], HERNÁNDEZ-MENA, Leonel*[1]

[1]*Centro de Investigación y Asistencia en Tecnología y Diseño del Estado de Jalisco A.C., Unidad de Tecnología Ambiental*
[2]*Universidad Tecnológica de Jalisco, División de Química Aplicada*

ID 1er Autor*: Valeria, Ojeda-Castillo* / **ORC ID:** 0000-0002-1397-0589, **CVU CONACYT ID:** 417629

ID 1er Coautor: *Perla Berenice, Sánchez-Torres* / **ORC ID:** 0000-0003-3646-2111, **CVU CONACYT ID:** 666703

ID 2do Coautor: *Leonel, Hernández-Mena* / **ORC ID:** 0000-0001-9120-5527, **CVU CONACYT ID:** 42463.

DOI: 10.35429/H.2020.8.1.23

V. Ojeda, P. Sánchez y L. Hernández

*lhernandez@ciatej.mx

A. Marroquín, J. Olivares, L. Cruz y A. Bautista. (Coord) Ciencias ambientales, uso de recursos. Handbooks-©ECORFAN-México, Querétaro, 2020.

Resumen

Las partículas finas (<1 micrómetro o PM_1) pueden tener efectos adversos sobre la salud humana debido a su tamaño y composición. Se colectaron muestras de PM_1 en dos sitios (Centro y Tlaquepaque) del AMG durante la temporada de secas cálidas, se analizaron para determinar concentraciones de aniones y cationes mediante cromatografía de iones. Los niveles de PM_1, ∑Aniones, $HCOO^-$, Cl^-, NO_3^-, SO_4^{2-}, $C_2O_4^{2-}$, ∑Cationes, Na^+, NH_4^+, K^+, Ca^{2+}, y Mg^{2+} sugieren concentraciones homogéneas en los dos sitios. Las especies más abundantes en cada sitio son SO_4^{2-}, NH_4^+, NO_3^-, Na^+, y K^+. Las fuentes secundarias de SO_4^{2-}, NH_4^+, y NO_3^- sugieren que los gases precursores (SO_2, NO_x, y NH_3) contribuyen significativamente a las concentraciones de iones en PM_1. El oxalato muestra una fuerte correlación con K^+, a partir de la quema de biomasa, y los principales iones secundarios ($\sum SO_4^{2-}$, NH_4^+, NO_3^-), por procesos de formación secundarios. La correlación negativa entre Na^+ y Ca^{2+} indica una fuente antropogénica. El balance de iones, la alta cantidad del total de cationes en el área de estudio, la comparación entre NH_4^+ observado y calculado, y la relación de amonio total/sulfato total (pendiente >5.99) son evidencia de condiciones ricas en amoníaco (ambiente alcalino). Los resultados de este estudio son las primeras caracterizaciones químicas de PM_1, incluido su contenido de aniones y cationes, de la segunda área urbana más grande de México.

Partículas finas, PM_1, Iones, Alcalino, Fuentes

1 Introduction

The particulate matter (PM) of outdoor air varies in size, shape, and chemical composition (Wenger et al., 2009). Whitby (1978) stated that fine particles are those <1 micron (also called PM_1) and may either be primary particles (such as diesel soot) or secondary particles formed by precursor gases. The secondary particles are formed through the nucleation of gas-phase compounds with low or non-volatility, from biogenic or anthropogenic sources, followed by the growth of a small particle. Nucleation and the subsequent growth processes influence the total number of particles and the size distribution, as well as the chemical and optical properties of the atmospheric aerosol. Coarse, fine, and ultrafine particles are generated by different processes. This suggests that each size has a particular composition of chemical species, allowing inferences about their emission sources and formation processes (Harrison et al., 2004; Whitby, 1978).

The properties of airborne particles—such as size distribution and chemical composition—are essential for assessing their adverse impacts on human health and their effects on visibility in urban areas. Therefore, some researchers propose using PM_1 as the pollution standard for air quality because it may provide more information about the sources of pollution than $PM_{2.5}$ and the association between fine particles and lung cancer and other cardiopulmonary diseases.

Numerous studies have determined ionic species in PM. However, the mass size distribution of water soluble inorganic and organic species is not well understood. Information about species such as sulfate, nitrate, ammonium, and other species in aerosol remains a significant knowledge gap (Tsai, Lin, Yao, & Chiang, 2012). Additionally, few studies have included new information about the distribution and secondary formation of ionic species. For example, sulfate and some organic compounds have a strong presence in fine particles (Pateraki et al., 2014) because of their formation through homogeneous nucleation. Tsai, Sopajaree, Chotruksa, Wu, & Kuo (2013) suggest that high amounts of sulfate could be associated with photochemical formation, related to anthropogenic activity and photochemical reactions. Other works (Yan et al., 2015) stated that physical and chemical characteristics of PM_1 are particularly significant for understanding fog formation and particle scavenging processes, particularly for secondary transformation. The fine particles' chemical composition includes inorganic species (e.g., ammonium, nitrate, and polar organic compounds) originating from the coagulation of ultrafine particles. However, organic species are a substantial fraction of the total mass of fine particles in the troposphere, ranging from 20% to 90% (Finlayson-Pitts & Pitts, 2000; Squizzato et al., 2016).

Understanding the concentrations, chemical compositions, and sources of fine atmospheric particles are essential for evaluating air quality, especially in cities with higher population density and elevated exposure to air pollutants. This work aims to determine the chemical composition of inorganic and organic ion species associated with PM_1 in the Guadalajara Metropolitan Area (GMA) in Jalisco, Mexico. This study is the first to determine the importance of sulfate, nitrate, and ammonium as chemical components of fine particles that can then be used to explore the origins of these components during days with high solar radiation.

2 Methodology

2.1 Sampling sites

Particle collection was conducted during the warm-dry season (April-June 2015) at two sampling sites. The first sampling site was the city center (CEN), located in the downtown area of the GMA (20° 40' 25" N; 103° 19' 59" W), which is characterized by significant vehicular and commercial activity. The second sampling site was Tlaquepaque (TLA), located in the southeastern direction from the CEN (20° 38' 27" N; 103° 18' 45" W), which is characterized by residential areas with major avenues and effects from industrial zones to the southwest (Figure 1.1).

Figure 1.1 Location of the PM_1 sampling sites at the CEN and TLA in the Guadalajara Metropolitan Area during the warm-dry period

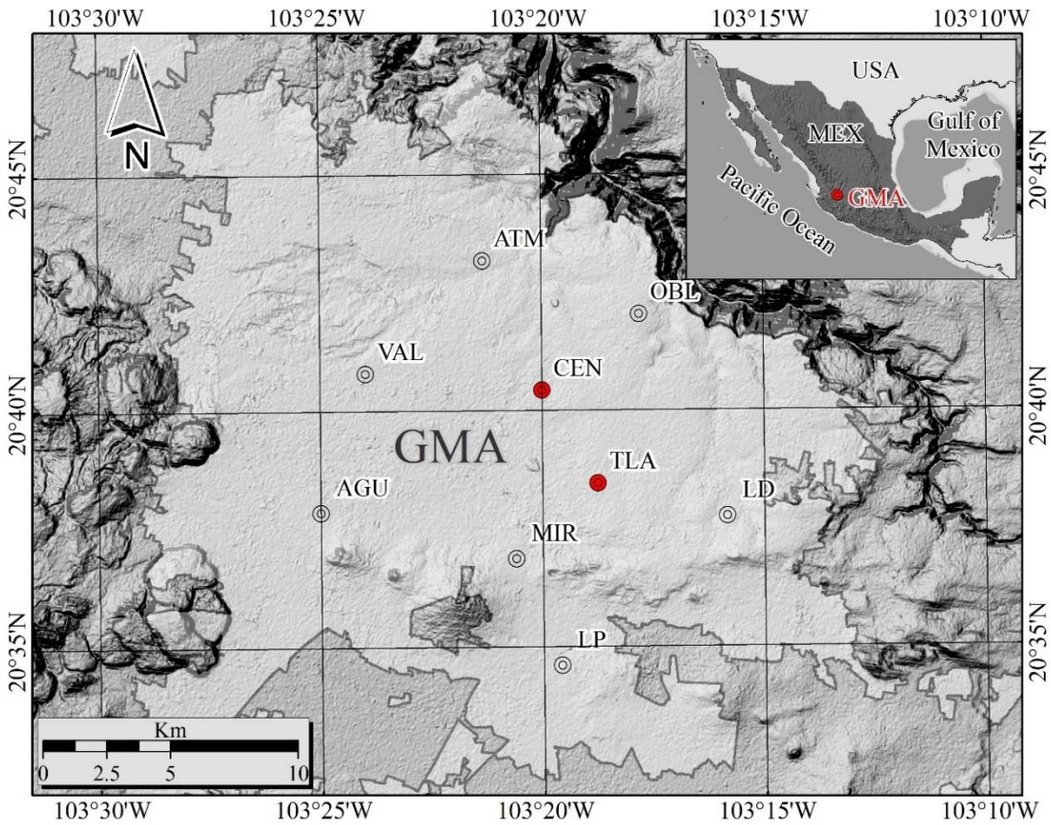

Source: (Ojeda-Castillo et al., 2019)

2.2 Particles collection and gravimetric analysis

Sets of 14 and 13 samples of PM_1 were collected in the CEN and TLA, respectively, starting at 00:00 h for 24 h with three-day intervals between samplings. Partisol Samplers (Model 2300, R & P) with multi-channels were used at both sites so that simultaneous samples could be collected. The samplers were programmed to a flow of 16.7 L/min. One channel was used for the gravimetric analysis utilizing a polytetrafluoroethylene (PTFE)-coated cartridge inlet with a PM_1 impactor (ChemComb 3500), equipped with a PTFE filter (46.2 mm diameter, Whatman) for PM_1 collection. The particulate mass was determined gravimetrically by pre- and postconditioning the sample for 24 h at a relative humidity of 38% (±4%) and mean temperature of 21 °C (±0.4 ºC) in an analytical microbalance (Sartorius SE2- F, with sensitivity 0.0001 mg). Another channel with the same types of inlet and flow cartridges but using nylon filters (diameter 47 mm, Magna) was used to collect particulate matter to determine the organic and inorganic ions. Filters were conditioned as described previously. Laboratory filter blanks and field filter blanks were also included on the sampling days. All sampling filters were transported and stored at 4 ºC until sample treatment. The results of the gravimetric analysis were expressed as $\mu g/m^3$.

2.3 Aqueous extraction with ultrasonic bath

The nylon filters were extracted in an ultrasonic bath (Branson 5510) for one h and 23 ºC, placing them in PP tubes (polypropylene) with ten mL of deionized water. The extracts, once obtained, were filtered through nylon membranes of 0.45 micrometers diameter pore to reduce the presence of particles. Subsequently, the extracts were transferred to injection tubes for analysis by Ion Chromatography.

2.4 Anions and cations in aqueous extracts from PM_1

The determination of the anions and cations present in the aqueous extracts from the PM_1 was performed by ion chromatography. Chemical and electronics suppression for anions was used, and only electronic suppression for cations (Advanced Compact IC 861, Metrohm), coupled with a conductivity detector and autosampler (Advanced Sample Processor 838, Metrohm). For anions, a Metrosep A Supp5_150 (Metrohm) column was used with sodium carbonate-sodium bicarbonate (3.2:1 mM) as the mobile phase at a flow rate of 0.7 mL/min (9.6 MPa, 35 ºC, and 20 min). A Metrosep C2_150 (Metrohm) column was used for cation analysis; tartaric acid-dipicolinic acid solution (4.1:0.8 mM) was used as the mobile phase at a flow rate of 0.9 mL/min (10.3 MPa, 35 ºC, and 20 min). The anion and cation standards considered in this study were CH_3COO^- (acetate), $HCOO^-$ (formate), Cl^-, NO_2^-, Br^-, NO_3^-, PO_4^-, SO_4^{2-}, $C_2O_4^{2-}$ (oxalate), Li^+, Na^+, NH_4^+, K^+, Ca^{2+}, and Mg^{2+}; all at a higher purity (99%-100%) or ACS grade (High-Purity Standards). The identification of these species in the PM_1 extracts was performed by matching individual standards retention times without exceeding a variation of ±5% (min). Anion and cation quantifications were done by injecting multi-standard and multilevel calibration solutions (0.15 to 10 µg/mL) by triplicate. The calibration results were analyzed using weighted linear regression, and the results showed that there was a significant correlation between the concentration (µg/mL) and the increase in conductivity (µS/cm·s) for every analyte (r >0.992 with $p<0.00001$ in all cases). For quality control, the total mass of the analytes (µg) was corrected for recoveries, extraction volume, laboratory filter blanks, and field filter blanks as proposed elsewhere (Hernández, Gallardo, Díaz &Villegas, 2017). The limits of detection (LoD) and limits of quantitation (LoQ) for every analyte were estimated from the linear regression. The LoD for anions ranged between 0.10 and 0.44 ppm (CH_3COO^- and NO_3^-, respectively), whereas the LoQ ranged between 0.21 and 3.13 ppm (CH_3COO^- and Cl^-, respectively). The LoD for cations was between 0.07 and 0.47 ppm, and the LoQ was between 0.14 and 0.94 ppm (for both Li^+ and K^+, respectively). All PM_1 extracts were injected in duplicate. The results of anions and cations were expressed as $\mu g/m^3$.

2.5 Meteorological parameters

During the sampling campaigns, meteorological parameters such as temperature (average, maximum and minimum; in Celsius degrees), relative humidity (RH; %), wind direction (WD), wind speed (WS, correspond to the mode; in m/s), maximum wind speed (MWS, correspond to mode; in m/s), atmospheric pressure (AP, mmHg), solar radiation (SR; W/m^2), 24 h maximum solar radiation (MaxSR; W/m^2), UV radiation, and maximum UV radiation (MaxUV; W/m^2) were registered (Vantage Pro2 Plus, Davis) every 10 minutes at the two sampling sites. The time series of these variables enabled the daily descriptive statistics to be calculated. For wind direction and wind speed, the most frequent data were reported for the period.

2.6 Statistics analysis

The *Shapiro-Wilk* normality test was used for the data sets of the study variables, which demonstrated the absence of normality. Because of this, nonparametric statistics were used to analyze the results. For the *intersite* analysis, PM_1, anions, cations data, and meteorological variables were contrasted using the *Mann-Whitney* test. Comparisons of ion species in one place (i.e., *intrasite*) were made using the *Kruskal-Wallis* test. The correlation analysis with *Spearman's rho* was applied to the data sampling site or the whole of both sites as a single set of results because of the absence of significant differences in most of the variables studied (the latter case will be referred to as *study area*). Linear regression analysis by least squares was used to demonstrate the existence of chemical processes, such as the neutralization between anions and cations present in the particles, and to estimate the levels of the coefficient of determination (r^2) between some of the variables. All these tests were performed using *Statistica* software v6.

3. Results and Discussion

3.1 Variations of the particle matter

Descriptive statistics of the PM_1 concentrations during the total sampling period at both sites are shown in Table 1.1, and the daily variation is shown in Graphic 1.1a. Although there were some increases in particles between days 42,141 and 42,158 in the CEN, there were no *intersite* differences ($p>0.18$) (Graphic 1.1b), probably because of a higher variation of PM_1 in the CEN.

Table 1.1 Descriptive statistics of PM_1 and anions-cations concentrations at the Guadalajara Metropolitan Area during the warm-dry period.

CEN (µg/m³)						
	n	**Mean**	**S.D.**	**Median**	**Maximum**	**Minimum**
PM_1	13	30.92	13.39	25.15	56.24	19.42
$HCOO^-$	13	0.12	0.02	0.11	0.16	0.09
Cl^-	1	0.19	--	0.19	--	--
NO_3^-	13	0.49	0.24	0.42	0.89	0.18
SO_4^{2-}	13	1.17	0.61	1.33	1.91	0.23
$C_2O_4^{2-}$	13	0.14	0.04	0.14	0.19	0.08
∑Ani	13	1.92	0.83	2.01	2.90	0.58
∑Ani/PM_1*	13	6.44	2.55	5.88	10.65	2.84
Na^+	13	0.62	0.10	0.58	0.82	0.50
NH_4^+	13	1.18	0.71	1.27	2.03	0.04
K^+	13	0.60	0.36	0.50	1.63	0.22
Ca^{2+}	13	0.31	0.15	0.29	0.77	0.20
Mg^{2+}	4	0.05	0.04	0.04	0.10	0.02
∑Cat	13	2.72	1.10	2.70	5.07	1.29
∑Cat/PM_1*	13	9.08	2.55	9.02	13.91	6.27
(∑Ani+∑Cat)/PM_1*	13	15.52	4.99	13.42	24.56	9.18
TLA (µg/m³)						
	n	**Mean**	**S.D.**	**Median**	**Maximum**	**Minimum**
PM_1	14	21.80	8.37	22.26	34.28	8.73
$HCOO^-$	14	0.11	0.03	0.10	0.18	0.08
Cl^-	5	0.21	0.04	0.21	0.27	0.17
NO_3^-	14	0.41	0.17	0.39	0.73	0.20
SO_4^{2-}	14	1.06	0.56	1.11	2.04	0.21
$C_2O_4^{2-}$	14	0.13	0.04	0.13	0.22	0.08
∑Ani	14	1.71	0.73	1.69	2.89	0.57
∑Ani/PM_1*	14	8.78	4.93	7.70	21.74	2.61
Na^+	14	0.76	0.29	0.62	1.30	0.45
NH_4^+	14	1.12	0.65	1.12	2.14	0.09
K^+	14	0.52	0.21	0.48	0.94	0.25
Ca^{2+}	14	0.30	0.13	0.26	0.56	0.10
Mg^{2+}	5	0.07	0.01	0.07	0.09	0.05
∑Cat	14	2.73	1.14	2.62	5.00	1.02
∑Cat/PM_1*	14	13.98	7.02	10.84	27.80	5.75
(∑Ani+∑Cat)/PM_1 *	14	22.76	11.79	18.10	49.54	8.36

*Ratio; ∑Ani: sum anions; ∑Cat: sum cations; S.D.: standard deviation.
Source: Own elaboration.

Graphic 1.1 (a) Concentration of PM_1 sample collected over 24 h in the CEN and TLA; **(b)** Particle concentration between sites (p>0.05). Box and Whisker plot represents minimum, 1st quartile, median, 3rd quartile, and maximum values of PM_1 concentration

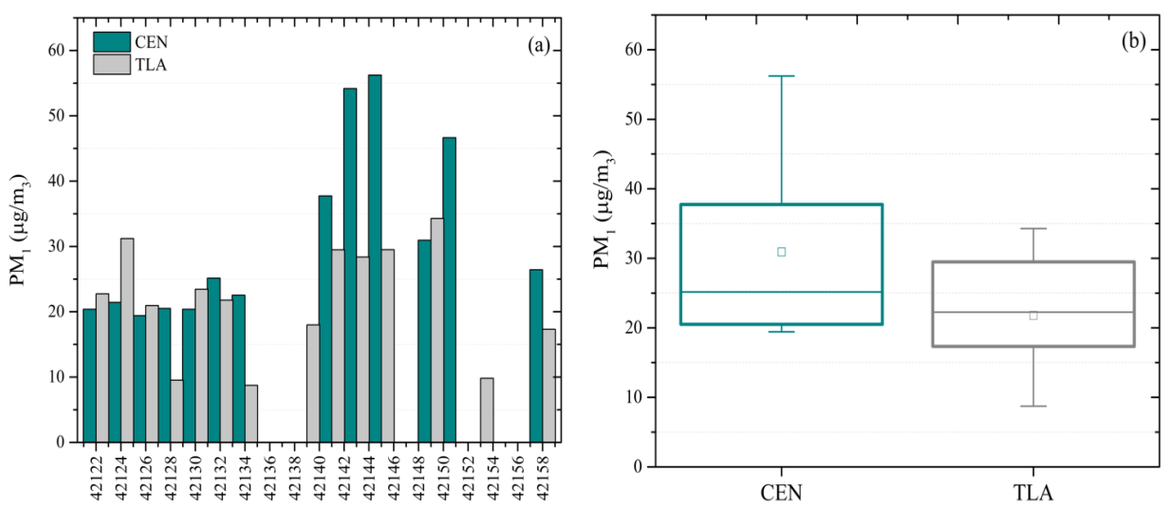

Additionally, the particles at both sites showed a weak correlation (r=0.44, p>0.05), which suggests that they may be influenced by the different types of local sources that determine the daily variation of PM_1 in the air. These results suggest homogeneous concentrations of particles in ambient air from the CEN to TLA (i.e., the downtown area to the southeast of the city). The close of the sites or the atmospheric stability conditions of the warm-dry period could partially explain these results. Wang, Zhuang, Sun, & An (2006) reported that the intensity of the emission sources could mainly control the fine particles' variation, even more so than the meteorological conditions. Likewise, Titos, Lyamani, Pandolfi, Alastuey, & Alados-Arboledas (2014) suggested that the concentration of particulate matter in a specific location depends on a great number of factors, such as local and regional sources of particles, as well as meteorological and geographical conditions. Minguillón, Querol, Baltensperger, & Prévôt (2012) proposed that low coefficients between the levels of PM_1 at two distant sites during the summer could also be attributed to a small number of data points and low particle concentrations in the air, which make them more susceptible to being influenced by local emissions.

The PM_1 median of the standard concentration in ambient air at the CEN and TLA were 25.15 and 22.26 $\mu g/m^3$, respectively. Table 1.2 shows the PM_1 levels reported for other cities in the world, which are highly variable depending on the type of population (urban or rural) and the sampling season. Higher particle concentrations occur in winter periods in some cities, suggesting that this behavior can be partially explained by the stability of atmospheric conditions (Agudelo-Castañeda & Teixeira, 2014). Data from Mexico City and other regions of the world provide a reference level of PM_1 for the GMA, but with the appropriate precautions by different situations, such as climatic conditions, season sampling, emissions intensity, number and type of sources, and particle measurement techniques.

Table 1.2 Concentration of PM_1 reported for different studies and cities

Country	City	Season	PM_1 ($\mu g/m^3$)
Switzerland (Minguillón et al., 2012)	Zurich (Urban) Payerne (Rural)	Winter Summer Winter Summer	17 7 12 6
China (Huang et al., 2013; Zhang et al., 2015)	Yangtze River Delta	Winter (2013) Winter (2010)	63 42
Spain (Titos et al., 2014)	Granada (Urban)	Annual (2006-2010)	17
Austria (Gomiščeк et al., 2004)	Vienna (Urban) Linz (Urban) Graz (Urban) AUPHEP-2 (Rural)	Winter Summer Winter Summer Winter Summer Winter Summer	15.5 14.2 17.6 11.9 20.9 14.1 12.1 12.8
Brazil (Agudelo-Castañeda & Teixeira, 2014)	Porto Alegre (Canoas-Urban) Porto Alegre (Sapucaia do Sul-Urban)	Winter Summer Winter Summer	11.6 8.6 17.5 13.5
Mexico (Guerrero, Alvarez, Retama, López, Castro & Salcedo, 2017)	Mexico City (urban)	Winter	27.8

Source: Own elaboration

3.2 Anions and cations from PM_1 aqueous extracts

Table 1.1 shows the descriptive statistics of the ion concentrations in the PM_1 aqueous extracts for the CEN and TLA. The *intersite* comparison for each ion (except Cl^-) indicates that the concentrations are non-different ($p>0.5$, all cases), suggesting uniformity in the content of the chemical species identified in PM_1 from the two sites at the GMA. The result is consistent with fine particle homogeneity in ambient air from the CEN and TLA. The *intersite* comparisons indicated that the sum of the anions and sum of the cations (ΣAnions and ΣCations, respectively) are equal ($p=0.66$ and $p=0.96$, respectively). Additionally, ions from both sites showed a strong correlation ($0.95>r>0.85$, all cases with $p<0.05$, except for Na^+, Cl^-, $Ca^{2+,}$ and Mg^{2+}), suggesting that similar local sources formed them. The *intrasite* comparison for the CEN and TLA suggests that ΣAnions and ΣCations are equal ($p>0.05$, both cases). However, when both variables are compared for the *study area*, the result is different and more reliable with high cation concentrations ($p<0.003$). The higher cation concentrations in the PM_1 aqueous extracts suggest a probable effect on the pH of the particles.

Concerning to the individual ions, SO_4^{2-} and NH_4^+ showed the highest concentrations at both locations, with their medians oscillating between 1.1 and 1.3 $\mu g/m^3$. Other abundant ions at the two sites were Na^+, K^+, and NO_3^-. At both locations, no significant *intrasite* difference was determined among these five species ($p>0.5$ in all cases), which makes them equally important in contributing to PM_1 under these sampling and analysis conditions. To complement these results, species such as $HCOO^-$ (formate) and $C_2O_4^{2-}$ (oxalate) showed medians less than 0.14 $\mu g/m^3$ at both sites without *intrasite* differences ($p>0.05$ in both cases). Magnesium showed a median of <0.07 $\mu g/m^3$ at both sites, whereas the Ca^{2+} concentration was 0.29 and 0.26 $\mu g/m^3$ in the CEN and TLA, respectively. Although the five most abundant species (SO_4^{2-}, NH_4^+, Na^+, K^+, and NO_3^-) showed significant differences from the least abundant species ($HCOO^-$, $C_2O_4^{2-}$, Ca^{2+}, and Mg^{2+}), no significant difference was found at least in one comparison. These results allow the most abundant ions to be defined with the PM_1 in ambient air at the GMA.

The above results (expressed in percentages) provide a better understanding of the contribution of the total ion sum (ΣTI) and principal secondary ion sum (ΣPSI: SO_4^{2-}, NO_3^- and NH_4^+) determined in this study, as well as the contribution made by the ΣAnions and ΣCations, to PM_1 concentrations. The ΣTI at the CEN and TLA was 14.5% and 19.1%, respectively, whereas the ΣPSI contributed 12.9% and 8.6% to the fine particles at the CEN and TLA, respectively. The ΣPSI in this study was less than 20% reported by other authors (Squizzato et al., 2016; Titos et al., 2014) during the summer in Venice, Italy. In this report, the ΣAnions and ΣCations in the CEN contributed 42.9% and 57.1% to ΣTI, respectively, whereas, in TLA, they contributed 38.1% and 61.9%, respectively. The ΣPSI at the CEN provided 60.1% of ΣTI and 57.3% in TLA. Therefore, the contribution made by ΣPSI becomes more important to ΣTI, and its contribution is low concerning PM_1. These results agree with those previously reported by Minguillón et al. (2012), which suggested that secondary inorganic compounds (e.g., sulfates, nitrates, and ammonium) are mainly present in fine particles. Perrone et al. (2013) found that the dominant PM_1 species were SO_4^{2-}, NO_3^-, and NH_4^+ in the suburban area of Salento, Italy. Titos et al. (2014) suggested that secondary inorganic aerosols (SO_4^{2-}, NO_3^- and NH_4^+) were the main components of PM_1. In particular, sulfate levels are slightly higher in spring and summer (Querol et al., 1999) than in other seasons, which is probably related to intense solar radiation. In this study, sampling was conducted during a period in which temperatures and solar radiation levels are the highest (April-May) (Díaz-Torres et al., 2017), which explains the high levels of sulfate (one of the main species contributing to the secondary inorganic aerosols) associated with PM_1 in the CEN and TLA. Therefore, the most abundant ions associated with PM_1 in the GMA's ambient air correspond positively with results observed in other cities. These suggest that species such as SO_4^{2-}, NO_3^-, and NH_4^+ are secondary components of fine particles produced by the transformation of their precursors (e.g., SO_2, NO_2, and NH_3) (Wang et al., 2006; Zhang et al., 2015).

The chemical characterization of PM_1 suggests that species such as Na^+ and K^+ and their sources are also important in the formation of fine particles in the study area. The origin of Na^+ and K^+ could be related to different anthropogenic activities around the sampling sites. The K^+ is reported as a product of biomass burning at low concentrations, although their concentrations could increase during episodes of higher contamination (Engling et al., 2011; Tsai et al., 2013). The presence of Na^+ in urban areas may be related to specific industrial activities, as in the case of the glass industry (Minguillón et al., 2012).

The source of Na^+ in TLA may probably be related in part to the intense artisanal activity and glass manufacturing in the area, as well as the proximity of an industrial area located to the southwest (Figure 1.1).

Less abundant organic ions such as $HCOO^-$ (formate) and $C_2O_4^{2-}$ (oxalate)—from the group of monocarboxylates and dicarboxylates, respectively—were determined in aqueous extracts from PM_1, whereas CH_3COO^- (acetate) was below the LoD. Formate may result from direct biogenic and anthropogenic emissions (Glasius et al., 2000). However, an important part of this compound could be derived from secondary transformations (Tsai et al., 2013). Oxalate has been reported to be the most abundant in the group of dicarboxylate compound, because oxalic acid is the final product of the photochemical decomposition (secondary reactions) of other dicarboxylic acids in the atmosphere from biogenic and anthropogenic precursors (Hsieh, Chen, Wan, Tsai, & Tsai, 2008; Hsieh, Kuo, Chen, & Tsai, 2009; Lim, Carlton, & Turpin, 2005; Tsai, Hsieh, Weng, Ma, & Kuo, 2008; Tsai et al., 2013). Oxalate may be present in the emissions from burning biomass (Legrand et al., 2007) and even primary emissions from transport vehicles (Kawamuras & Kaplan, 1987). Laongsri & Harrison (2013) suggested that dicarboxylate concentrations are higher in fine particles, especially in aerosol samples from urban sites.

Both Ca^{2+} and Mg^{2+} (present in five and four samples at TLA and the CEN, respectively), have a mineral origin into coarse particles. Some direct sources that cause their presence are the resuspension of dust on unpaved avenues and streets and/or anthropogenic activities involving crushing geological materials (Aldabe et al., 2011; Tsai et al., 2013). The low concentration of Ca^{2+} and Mg^{2+}, as well as their low frequency in the fine particles of the CEN and TLA, and the greater abundance of sulfate, ammonium, and nitrate suggest that PM_1 are mainly of secondary origin.

Finally, Cl^- was found during only a few days at TLA, and its sources were intermittent or probably associated with other particle sizes. Related studies with different particle sizes of Cl^- (Huang et al., 2016; Wang, Zhuang, Chen, An, & Zheng, 2007) suggested that Cl^- could be derived from local industry emissions, biomass (coal) or waste burning. Other authors (Harrison & Yin, 2000) indicated that Cl^- in atmospheric particles result in neutralization between ammonia and HCl vapors. The latter of which comes from sources such as incinerators and power stations.

Table A1 shows an *intrasite* matrix of the *Spearman's rho* with the study variables. Correlation patterns are shown in the sampling sites. At the CEN, $HCOO^-$, NO_3^-, SO_4^{2-}, $C_2O_4^{2-}$, Na^+, NH_4^+, K^+, ΣAnions, and ΣCations had r values between 0.65 and 0.82 with PM_1 ($p<0.05$ in all the cases). In TLA, the same variables ranged from 0.28 to 0.49 with PM_1, all $p>0.05$. The values of r were significant when they were estimated for the *study area* (0.45 to 0.63, all $p<0.05$), highlighting the importance of sample size to define the relationship between the variables of interest. The r values of ΣPSI and ΣTI with PM_1 at the CEN were also significant when determined from the *study area* (all $p<0.05$). These latest results suggest that part of PM_1 at the CEN probably comes from biomass burning, vehicle emissions, biogenic emissions, or atmospheric secondary reactions. In TLA, the absence of significant relationships between PM_1 and some specific ions suggests that the organic component could better explain the variation of fine particles (∑oxalate+formate have $r=0.55$ with $p<0.05$ and at the CEN an $r=0.79$ with $p<0.05$). Other studies (Zhang et al., 2015) proposed the contribution of organic components ranging between 47% and 62% of the PM_1 (Pateraki et al., 2014).

In the case of the correlation between Ca^{2+} and PM_1, r was negative or very low ($p>0.05$) for both sites (with Cl^- and Mg^{2+} not being determined because of a lack of data), which suggests that PM_1 have scarce influence from emission sources that origin calcium and magnesium (e.g., geological or mechanical). Overall, Ca^{2+} showed low or negative coefficients with other ion species at both sites and in the *study area* (all $p>0.05$), which indicates that fine particles are mainly composed of secondary ions, and suggest that coarse particles have mineral components, especially Ca^{2+} and Mg^{2+} (Titos et al., 2014). These results provide guidelines for linear regression analysis using least squares to establish the coefficient of determination (r^2) to understand better how PM_1 variation depends on the presence of ions in the *study area* (Table 1.3). Anions explain a low variation of PM_1 ($r^2=0.30$, $p<0.002$), whereas the ΣCations was $r^2=0.39$ ($p<0.0007$). Additionally, the ΣPSI of $r^2=0.26$ ($p<0.006$) and ΣTI of $r^2=0.31$ ($p<0.002$) explain the variation of PM_1. With respect to individual ions and their relationship with PM_1, NO_3^- resulted in $r^2=0.27$ ($p<0.006$), SO_4^{2-} in $r^2=0.29$ ($p<0.003$), NH_4^+ in $r^2=0.23$ ($p<0.01$), Na^+ in $r^2=0.22$ ($p<0.02$), and K^+ in $r^2=0.49$ ($p<0.00004$).

The above results give specific evidence of the effect of some of the most abundant species of ions (NO_3^-, SO_4^{2-}, NH_4^+, Na^+, and K^+) on the variation of PM_1. These results suggest that the origins of these species are the likely sources of the concentration of fine particles in the *study area*. However, r^2 values are moderate to low, which allows the possibility that some other chemical species could better explain the variation of PM_1. For example, ∑oxalate+formate had r^2=0.40 ($p<0.0004$) in the *study area*.

Table 1.3 Regression analysis parameters of PM_1 and anions and cations in the *study area*

Study Area	Equation	r^2	p-value
∑Anions	$y = 1.92 + 8.43x$	0.30	<0.002
∑Cations	$y = 9.14 + 6.19x$	**0.39**	<0.0007
∑PSI	$y = 14.22 + 4.41x$	0.26	<0.006
∑TI	$y = 9.26 + 3.70x$	0.31	<0.002
NO_3^-	$y = 14.36 + 21.22x$	0.27	<0.006
SO_4^{2-}	$y = 13.75 + 11.18x$	0.29	<0.003
NH_4^+	$y = 16.39 + 8.50x$	0.23	<0.01
Na^+	$y = -0.99 + 44.16x$	0.22	<0.02
K^+	$y = 10.09 + 28.84x$	**0.49**	<0.00004
∑oxalate+formate	$y = -3.9 + 119.90x$	**0.40**	<0.0004

∑Ani: sum anions; ∑Cat: sum cations; ∑PSI: sum principal secondary ions; ∑TI: sum Total Ions.
Higher values in bold
Source: Own elaboration

3.3 Anions and Cations sources

Anions and cations have similar correlation guidelines at the individual sites (and in the *study area*), which highlights the relationship between the five main ions (NO_3^-, SO_4^{2-}, NH_4^+, Na^+, and K^+). The data (Table A1) suggest that there are common sources, via either direct emission or secondary atmospheric chemical processes, for the origins of these ions in PM_1. Based on these observations, some simple estimates can be made to increase the evidence of potential emission sources. For example, moderate *r* values were observed between the presence of SO_4^{2-} and NO_3^- at both sites. The NO_3^-/SO_4^{2-} ratio (in mass) could be used to assess the relative importance of stationary and mobile sources, assuming that NO_2 comes from vehicle emissions and contributes to the formation of NO_3^- and that SO_2 comes from coal combustion and is usually converted to SO_4^{2-} in urban atmospheres (Yan et al., 2015). A high NO_3^-/SO_4^{2-} ratio will occur when motor vehicle emissions exceed coal-burning emissions (Du et al., 2011). In the CEN and TLA, the medians of NO_3^-/SO_4^{2-} ratio were <0.5 with maximum values at both sites between 0.76 and 0.93, respectively. These values preliminarily suggest that mobile sources and their emissions are not high at these sites. However, these data should be viewed with caution because the NO_3^- and SO_4^{2-} levels were not different ($p>0.05$) and provided a similar contribution to the PM_1 concentration at both sites. A study by Zhang et al. (2015) reported a ratio of 0.96 on low pollution days and 1.64 on high pollution days. A likely explanation for the lower NO_3^-/SO_4^{2-} ratio in the GMA is the low thermal stability of NH_4NO_3 during periods of high temperature, which promotes its dissociation from fine particles or favors the formation of gaseous HNO_3 (Aldabe et al., 2011; Guo et al., 2010; Laongsri & Harrison, 2013). A more precise estimate of NO_3^-/SO_4^{2-} ratio from vehicle emissions in the GMA could probably be obtained if the contribution of NO_x in the formation of NH_4^+ was considered. The NO_x are transformed into HNO_3 (nitric acid) by oxidation and the subsequent reaction with NH_3 (ammonia) to form ammonium nitrate (median of the $NO^{3-}+NH_4^+/SO_4^{2-}$ ratio = 1.39 with a maximum of 2.12 in the *study area*) (Finlayson-Pitts & Pitts, 2000). This estimation does not include the contributions of soil and some agricultural activities to NH_4^+ and does not rely on the assumption that this contribution is low in urban areas. Moreover, NH_4^+ particulates in the fine fraction are mainly formed secondarily, whereas, in the coarse fraction, they are mostly derived from suspended soil that contains fertilizer (Wang et al., 2013). The latest vehicle fleet data have been reported to be 1.84 million vehicles in the GMA (INEGI, 2010). We assume that the vehicle emissions have a more significant impact on the atmosphere, which is an inconsistent condition with the low NO_3^-/SO_4^{2-} ratios in the study sites.

Other important relationships were observed in the CEN, where SO_4^{2-} had values r=0.87 and r=0.80 with ammonium and oxalate, respectively. In TLA, these correlations showed higher values (r=0.96 and r=0.90, same order). The relationship between NH_4^+ and SO_4^{2-} could be explained because both have a secondary origin from precursors of direct combustion emissions (NOx and SO_2). Based on this relationship, Zhang et al. (2015) reported r=0.93 between $SO_4^{2-}$and NH_4^+ near Hangzhou, Shanghai, and Nanjing in China, particularly on high pollution days. The relationship between sulfate and oxalate suggests that the organic species have a probable origin in secondary reactions (Yang et al., 2014). For oxalate, this is supported by the r values ($p<0.05$) with NO_3^- and NH_4^+. The high correlation between oxalate and sulfate is evidence of a similar process to the formation of dicarboxylate (Feng et al., 2012; Yang et al., 2014). Based on this correlation, Langner & Rodhe (1991) found that 80% of sulfate is formed in the global atmosphere from chemical processes occurring in the clouds. This last result provides guidelines for analyzing the linear regression between oxalate and ΣPSI, with r^2=0.91 in the CEN and r^2=0.79 at TLA, respectively. Graphic 1.2a shows the results of the same analysis for the *study area*, with r^2=0.86 ($p<0.05$). This result is evidence of a probable secondary origin of oxalate. Based on this, Laongsri & Harrison (2013) found high r between oxalate and sulfate at $PM_{2.5}$ and suggested that this may be because of secondary atmospheric processes. Additionally, these authors found that both ions are distributed similarly in fine particles of different sizes.

Furthermore, Tsai et al. (2013) note that $C_2O_4^{2-}$ and SO_4^{2-} in aerosols are final products of organic and inorganic species, and that the $C_2O_4^{2-}/SO_4^{2-}$ ratio (in mass) provides information for determining the formation of dicarboxylate from inorganic salts. A high $C_2O_4^{2-}/SO_4^{2-}$ ratio suggests an increase in the photochemical formation of oxalate. At the CEN, the median was 13.3%, and in TLA it was 12.5%, which are relatively low values (Graphic 1.2b) considering the mass of sulfate (in both sites days 42,128 and 42,130 were between 32% and 39%), although they are higher than the results reported by Hsieh et al. (2008) for $PM_{2.5}$ particles. These results suggest that only part of the oxalate (<13.3%) present in the PM_1 originate from secondary reactions in the atmosphere.

On the other hand, there is a strong r between the concentrations of $C_2O_4^{2-}$ and K^+ (Table A1), with K^+ being a specific marker of biomass burning. Regression analysis indicates that the oxalate explained 75% and 79% of the variation of K^+ (water-soluble) in the CEN and TLA (with r^2=0.76 in the *study area*, Graphic 1.2c). The results of these analyses suggest that a portion of oxalate can be attributed to direct emissions from biomass burning or even related to vehicular traffic emissions (Tsai et al., 2013). Although K^+ could have a geological origin (Tsai, Wu, Hsu, & Yang, 2010), the two sites showed a negative and low r ($p>0.05$) with Ca^{2+}, which is an indicator of this source (Tsai & Chen, 2006). This reaffirms their origin from direct emissions of burning biomass and probably the same source for a part of the oxalate in PM_1. Other authors have proposed potassium and oxalic acid as some of the main markers of biomass burning (Hsieh et al., 2008; Lee et al., 2011; Tsai et al., 2013).

Graphic 1.2 (a) Scatter plot and linear regression line between oxalate and ∑PSI concentration (sulfate, nitrate, and ammonium) in the *study area*; **(b)** The $C_2O_4^{2-}/SO_4^{2-}$ ratio (in mass) between sites (p>0.05). Box and Whisker plot represent minimum, 1st quartile, median, 3rd quartile, and maximum Oxalate/Sulfate mass ratio values; **(c)** Scatter plot and linear regression line between oxalate and K^+ (of biomass burning origin) in the *study area*

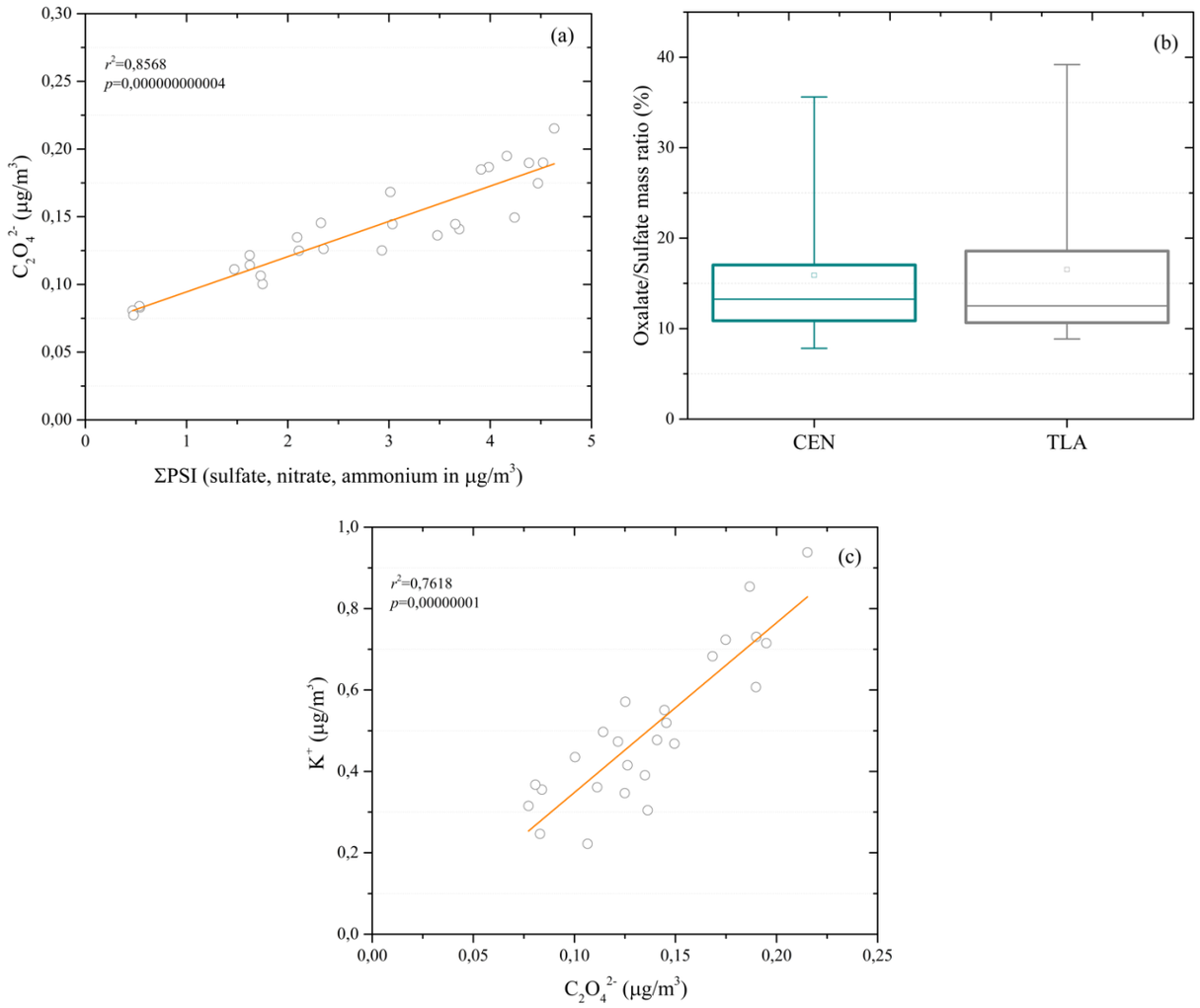

The Na^+ ion showed a negative *r* and low correlation with the Ca^{2+} in the CEN and TLA, suggesting that it does not have a geological origin. In contrast, sodium correlated with K^+ at the two sites (*r*=0.72 and *r*=0.89, both with p<0.05), as well as also with formate, nitrate (except TLA), sulfate, oxalate, and ammonium. All these are species that have proven secondary origins (nitrate, ammonium, sulfate), secondary source or direct emissions (format and oxalate), or sources for direct emission (K^+). These results suggest that Na^+ shares a common origin with any of these species or is an integrating compound with them. As indicated, Na^+ is likely related to the glass manufacturing industry, mainly in TLA.

Although it was not one of the most abundant, formate ion showed a medium to high correlation with oxalate at both sites and higher in the *study area* (*r*=0.83, p <0.05), which is similar to other organic ions. In the *study area,* formate also showed higher coefficients with ΣPSI and potassium, and lower coefficients with Na^+. These results are consistent with other studies that indicated that this species has a source from direct biogenic emissions and anthropogenic emissions (Glasius et al., 2000). However, it is possible that a significant part of this compound could have been derived from secondary transformations (Tsai et al., 2013).

Based on the positive *r* (p<0.05) between species with greater contribution to PM_1, it is probable that it could contribute to the formation of some chemical compounds. Sodium nitrate ($NaNO_3$), ammonium nitrate (NH_4NO_3), and potassium nitrate (KNO_3) would probably be present in the CEN; ammonium nitrate would be present in the TLA; and sodium sulfate (Na_2SO_4), ammonium sulfate [$(NH_4)_2SO_4$] and potassium sulfate (K_2SO_4) would be present at both sites.

3.4 Neutralization process in PM_1

The atmospheric chemical process of neutralization between anion and cation species was assessed using ion balance. The results of the least-squares linear regression analysis applied to ∑Anions ($HCOO^-$, $C_2O_4^{2-}$, NO_3^-, and SO_4^{2-}) and ∑Cations (Na^+, NH_4^+, K^+, Ca^{2+}, and Mg^{2+}) at µEq/m^3 (micro equivalent per cubic meter) (Koçak et al., 2007; Pateraki et al., 2014).

The slope in the CEN (2.24) and TLA (3.47) suggests that particles have a deficit in the amount of anion. The anion deficit avoids neutralization of species with basic or alkaline properties (e.g., NH_4^+, Ca^{2+}, K^+, and Na^+) in PM_1 (Jacobson et al., 2000; Pateraki et al., 2014). As shown in Graph 1.3a, the slope of the study area (2.88) indicates that the anion deficit of PM_1 scarcely neutralizes the cations and that this condition contributes to the alkaline character of the particles.

However, the results from ion balance could show slight variations with the number of chemical species included (some in the gas phase) (Moya et al., 2003). The results in this study show the alkalinity of the PM_1 particles from the ion balance and the presence of water-soluble species. The alkalinity of the particles agrees with the higher ∑Cations levels in *the study area* with respect to ∑Anions ($p<0.05$). Other works (Cheng et al., 2011; Squizzato et al., 2016) proposed and used a comparison between the observed and calculated NH_4^+ concentrations to assess the formation of secondary ions. The amounts of NH_4^+ can be calculated using stoichiometric ratios of the more abundant compounds (ammonium sulfate [$(NH_4)_2SO_4$], ammonium bisulfate [NH_4HSO_4] and ammonium nitrate [NH_4NO_3]). This calculation assumes that NO_3^- is present as NH_4NO_3 and SO_4^{2-} is in the form of $(NH_4)_2SO_4$ or NH_4HSO_4. The results of the observed and calculated NH_4^+ at the *study area* show that slope=0.33 when $(NH_4)_2SO_4$ is assumed and that slope=0.28 when NH_4HSO_4 is assumed (Graphic 1.3b). These slope values suggest that ammonium with higher availability neutralized fully to aerosols.

The latest results have a strong relationship with the total ammonium/total sulfate (TA/TS) molar ratio. The estimated TA/TS molar ratio has some suppositions and characteristics, as reported previously (Seinfeld & Pandis, 2006). For example, for TA/TS<2, the environmental conditions are defined as ammonium poor (acidic environment). When TA/TS>2, the environmental conditions are defined as ammonium rich (no-acidic or alkaline environment). In the *study area*, a TA/TS was found to be 5.99 (CEN=6.01 and TLA=6.04). The ratio values were equivalent to the slope of the linear regressions between SO_4^{2-} and NH_4^+ in µMol/m^3 (micromole per cubic meter). The molar ratio values suggest that fine particles have a high ammonium concentration, which is a condition that contributes to alkaline properties (Graphic 1.3c). The results of this study indicate higher NH_4^+ concentration, from which only a small portion is neutralized by sulfate in the PM_1. Other reports (Chung et al., 2001) have found that ammonium ion acts as the dominant cation in the fine particle fraction. The results for California indicate ultrafine particles are primarily alkaline (rather than acidic) in nature. It is possible that fine particles <1 µm in the GMA *study area* could be agglomerated from a large number of ultrafine particles with alkaline properties. There is currently limited knowledge of the potential adverse effects on human health by the inhalation of alkaline ultrafine particles (Chung et al., 2001).

3.5 Meteorological parameters and their relationship with the ionic species

Table 1.4 shows the descriptive statistics about meteorological parameters and their daily variation during the sampling period. Medians of the daily, maximum, and minimum temperatures and RH did not have *intersite* differences ($p>0.05$, all cases). The wind speed (WS) and maximum wind speed (MWS) in general were <3.1 m/s without significant differences ($p>0.05$, in both cases). The WS direction and MWS direction in the CEN originate from west and west-northwest, respectively. For TLA, both the WS and MWS directions come from the west. Atmospheric pressure, UV radiation, and MaxUV radiation had higher levels at the CEN ($p<0.00001$, $p<0.005$, and $p<0.00031$, respectively). The SR and MaxSR did not show the *intersite* differences ($p>0.05$, in both cases).

Graphic 1.3 (a) Scatter plot and linear regression line between ∑Cat and ∑Ani in the *study area*; **(b)** Comparison between calculated and observed ammonium in fine particles in the *study area* $(NH_4)_2SO_4$: calculated $NH_4^+ = 0.38 \cdot [SO_4^{2-}] + 0.29 \cdot [NO_3^-]$ and NH_4HSO_4: calculated $NH_4^+ = 0.192 \cdot [SO_4^{2-}] + 0.29 \cdot [NO_3^-]$; **(c)** Scatter plot and linear regression line between SO_4^{2-} and NH_4^+ in µMol/m^3 in the *study area*

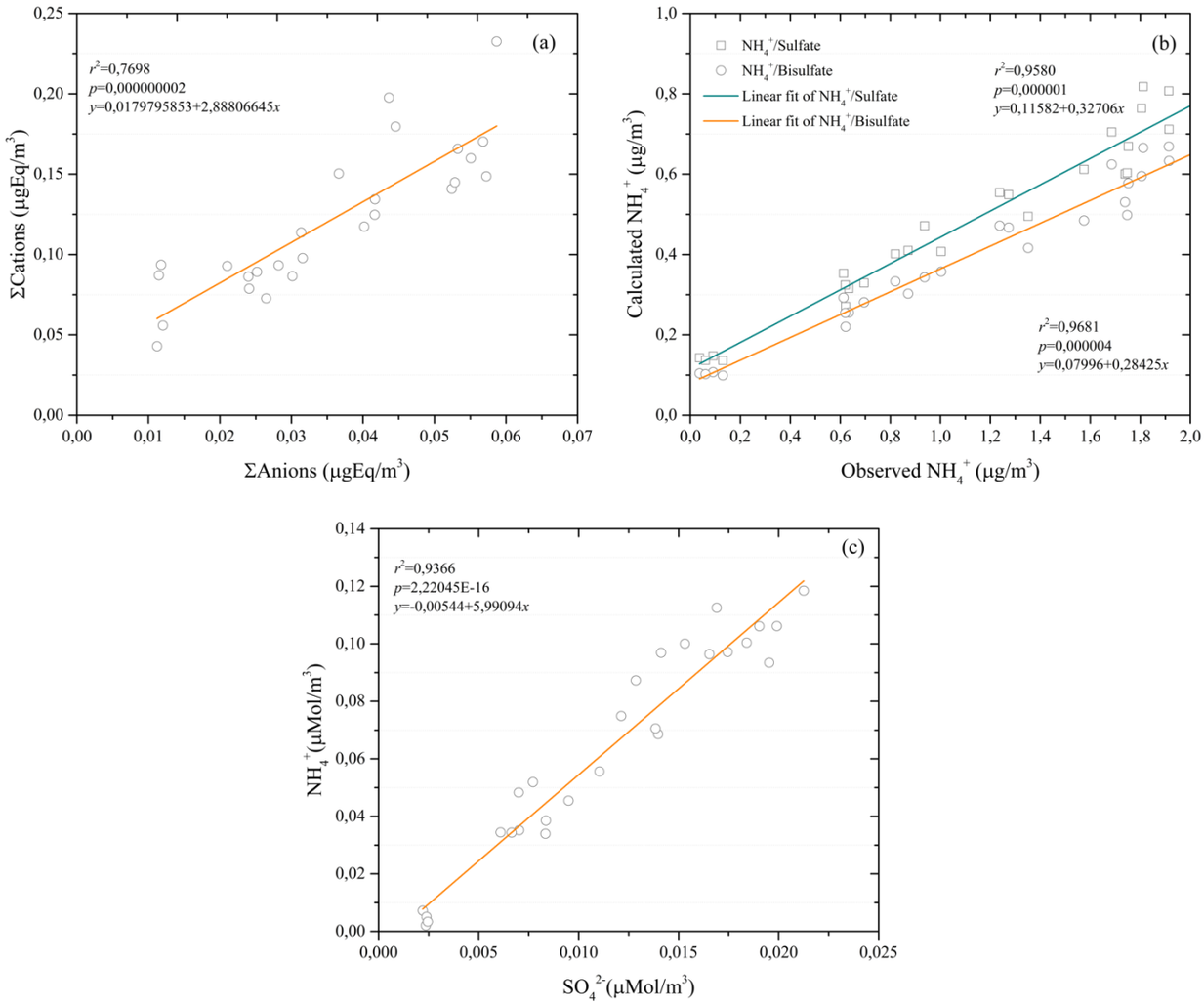

At the CEN and TLA, the *intrasite* and *intersite* patterns of correlation between meteorological parameters (Table A2) were observed. The results of the *intrasite* pattern correlation are $p<0.05$ in some cases. The *intersites* pattern correlation is highlighted by the frame cell in a diagonal line, with numerous coefficients having $p<0.05$ (except for WS and MWS). The results suggest that the sampling sites have similar physical environments—except for atmospheric pressure, UV radiation, and MaxUV radiation—and that there are weak correlations between wind speeds at both sites. The similarities and differences observed in the meteorological parameters and the pollutants related to PM_1 could be explained by geographical locale, altitude, and cloud presence during the sampling days. They could also be related to the thermal inversion and conditions that occur over several days in the GMA from January to June, which are less favorable to pollutant dispersion. The orographic and natural barriers around the GMA could also obstruct the normal wind flow and intensify pollutant stagnation (SEMARNAP-SS-SG, 1997).

No significant correlations between the PM_1 levels and the meteorological parameters were found for both sampling sites (except MaxSR and MaxUV at the CEN). Nevertheless, the temperature (average and minimum), MWS, and MaxSR for the *study area* showed *r* values with $p<0.05$ (Table A3). Other studies suggested that a relationship between PM_1 and temperature could exist because high temperature and solar radiation conditions combined with low relative humidity produce dry particles. However, no significant contributions to the particle mass in ambient air have been found from these conditions (Massey et al., 2012). It is not surprising that a significant correlation was observed for fine particles and MWS because of the well-known relationship among thermal inversion episodes, slow winds (in both sites <3.1 m/s), and poor vertical dispersions of pollutants because of thermal stability within air layers (Guzmán-Torres et al., 2009). Additionally, the MaxSR and MaxUV radiation showed negative *r* values with the fine particles at the CEN (in TLA, the estimated *r* values were low negative and showed $p>0.05$).

However, in the *study area*, only the MaxSR showed a negative coefficient with $p<0.05$. The carbon content could likely explain this situation in fine particles. Carbon is a component with the capacity to absorb a significant amount of solar radiation. The heat storage capacity of the particles and the surrounding air layers (Gaffney & Marley, 2009; Herrmann & Hänel, 1997; Marley et al., 2001) could affect the behavior of low thermal stable compounds (e.g., NH_4NO_3), and therefore promote particle mass loss (Aldabe et al., 2011; Laongsri & Harrison, 2013). These results suggest the need to generate more data to establish robust relationships between PM_1 and local meteorology, determine the hourly variation of ionic components associated with fine particles, and determine organic and elemental carbon.

Table 1.4 Descriptive statistics of the meteorological parameters at the Centro (CEN) and Tlaquepaque (TLA) sites during the warm-dry period

CEN						
	n	Mean	S.D.	Median	Maximum	Minimum
AT (ºC)	15	24.30	1.46	24.92	25.81	21.03
MT (ºC)	15	24.41	1.46	25.01	25.92	21.16
mT (ºC)	15	24.18	1.46	24.82	25.70	20.90
RH (%)	15	46.33	9.35	47.45	69.55	34.40
WS (m/s)**	15	0.9	--	0.90	2.70	0.00
WD**	15	W (10)	--	--	--	--
MWS (m/s)**	15	2.2	--	3.10	6.30	0.90
WDMWS **	15	WNW (4)-N (4)	--	--	--	--
AP (mmHg)	15	842.08	1.20	842.35	844.06	839.33
SR (W/h)	15	255.47	27.36	263.08	288.04	204.19
MaxSR (W/h)	15	987.67	60.98	966.00	1111.00	897.00
UV	15	2.38	0.29	2.44	2.76	1.83
MaxUV	15	10.89	1.20	11.10	8.60	12.90
TLA						
	n	Mean	S.D.	Median	Maximum	Minimum
AT (ºC)	14	24.61	1.306	25.01	25.94	20.79
MT (ºC)	14	24.73	1.30	25.13	26.06	20.91
mT (ºC)	14	24.49	1.31	24.89	25.82	20.66
RH (%)	14	45.33	10.46	45.22	70.76	33.99
WS (m/s)**	14	0.40	--	1.10	2.20	0.40
WD**	14	W (8)	--	--	--	--
MWS (m/s)**	14	3.10	--	3.10	4.90	0.90
WDMS**	14	W (8)	--	--	--	--
AP (mmHg)	14	835.57	1.21	835.76	837.55	832.82
SR (W/h)	14	262.50	26.70	263.83	308.78	217.66
MaxSR (W/h)	14	969.43	49.17	960.50	1049.00	871.00
UV	14	2.05	0.21	2.06	2.45	1.72
MaxUV	14	8.82	0.70	8.90	9.80	7.70

AT: average temperature (24 h); MT: maximum temperature; mT: minimum temperature; RH: relative humidity; WS: wind speed; WD: wind direction; MWS: maximum wind speed; WDMS: wind direction of maximum speed; AP: atmospheric pressure; SR: solar radiation; MaxSR: maximum solar radiation; UV: ultraviolet radiation; MaxUV: maximum ultraviolet radiation; S.D.: standard deviation. **Correspond to the mode in 24 h period.

Other studies have reported the relationship between particles and meteorological variables, which suggests that fine particles are most likely being controlled by local emissions rather than being influenced by meteorology (Pateraki et al., 2014; Wang et al., 2006). Titos et al. (2014) also suggested that for specific locations, particle concentrations would not only depend on the local and regional sources, but also geography.

The analysis of relationships between ionic species and meteorological parameters, RH was found to have a positive *r-value* ($p<0.05$) at the CEN for NO_3^-, $C_2O_4^{2-}$, K^+, and ∑Cations. Furthermore, RH was found to have a positive and significant *r* value for $HCOO^-$, NO_3^-, SO_4^{2-}, NH_4^+, ∑Anions, ∑Cations, and ∑PSI at TLA. When the correlation coefficients were estimated for the *study area*, all ionic species showed *r* values ranging from 0.51 to 0.64 with $p<0.05$, except for Na^+ and Ca^{2+}. In the CEN, MaxSR and MaxUV showed moderate to high negative correlations (all with $p<0.05$) for all ion species (except Ca^{2+} with both parameters and SO_4^{2-} with MaxUV). In TLA, the MaxUV variable showed a negative correlation (all $p<0.05$) with all ion species (except formate, sodium, and calcium).

The number of correlation coefficients showing significant values for variables—such as MaxSR, UV radiation, and MaxUV—increased in number at the *study area* (all with negative *r* values). The WS and MWS show moderate and positive correlation coefficients in TLA for nitrate, oxalate, ∑Anions, and ∑PSI, all with $p<0.05$ (the CEN showed *r* values with $p>0.05$ in all cases). However, in the *study area*, only MWS showed *r* values ranging from 0.39 to 0.46 for NO_3^-, $C_2O_4^{2-}$, ∑Anions, and ∑PSI (all positive and $p<0.05$).

For the relationships of NO_3^- and SO_4^{2-} with RH, Zhang et al. (2015) suggested that high levels of relative humidity contributed to a rapid increase of secondary inorganic species at episodes of severe pollution. Other authors (Turšič et al., 2004) have also proposed that oxidation of SO_2 to SO_4^{2-} in the particle's surface area occurs mainly when RH is high. Li, Zhu, Zhao, Zhang, & Chen (2010) stated that under conditions of high RH, the transformation ratio from NO_2 to NO_3^- with the interaction of preexisting particles was higher when compared with the process occurring at low RH values. The maximum RH at both sampling sites ranged from 50% to 70% during some days, and it is possible that their positive relationship with NO_3^- and SO_4^{2-} could be explained by such descriptions. Huang et al. (2016) suggested that the effects of high temperature and RH on fine particles would facilitate the secondary formation of ammonium sulfate and ammonium nitrate, and we also found a significant correlation between RH and NH_4^+ with $r = 0.56$, $p<0.05$ in the *study area*.

Results for MWS suggest that the variation of secondary ionic species is probably related to the air mass transport between sites, mainly on days with high wind speed from the west and west-northwest. Wang et al. (2007) found a negative correlation between wind speed and $HCOO^-$, which suggests local sources as the main origin for $HCOO^-$, whereas a positive correlation between wind speed and CH_3COO^- indicates a process of transport from a distant location. In this study, positive *r* values were observed for MWS and all anions species (except calcium) in the *study area*.

In the *study area*, a negative correlation between nitrate with SR, MaxSR, UV radiation, and MaxUV (all with $p<0.05$) was found. The nitrate in the particles, specifically the ammonium nitrate, has low thermal stability and its loss could occur if compounds such as carbon, related with an increase in temperature, are presents (Gaffney & Marley, 2009; Herrmann & Hänel, 1997; Marley et al., 2001). According to the results of this study, it is probable that SR and UV radiation could have the same effect on other ion species. Additionally, nitrate and temperature showed a negative correlation coefficient (not significant in both sites). The meteorological analysis and its relationship with the ionic composition of PM_1 at the CEN and TLA showed the role of meteorological parameters in the ionic composition variation of PM_1 in ambient air.

4 Conclusions

Fine particles (PM_1) at two study sites in the GMA suggest homogeneity in their ambient air concentrations. Meteorological parameters showed similar values between sites (except atmospheric pressure and UV radiation), and the temperature was identified as the variable with the most influence on the particle's concentration levels. Low or absent correlations with other meteorological parameters suggest that local emission sources better explain the variations in the particle's nature. Sulfate, nitrate, and ammonium were found to be the principal secondary ions (PSI), highlighting the crucial role of atmospheric transformation processes (and the sodium and potassium from direct emissions) on the formation of fine particles at the CEN and TLA.

In relation to oxalate, a significant correlation with K^+—which is a marker of biomass burning—and PSI (sulfate, nitrate, and ammonium) was observed, suggesting two different origins. The PSI values also had equal levels at both sampling sites (like fine particles) under the sampling conditions tested. The ion balance between ∑Anions and ∑Cations indicated fine particles with alkaline properties in the CEN and TLA, from a higher amount of cations. This agrees with the relationship between the observed and calculated NH_4^+ and with the AT/ST ratio assessed (>5.99), which suggests ammonium rich particles. Ion species showed positive correlation coefficients, mainly with RH and MWS, and negative correlations with MaxSR and UV radiation. Based on the high *intersite* similarity of the meteorological parameters and the moderate variability that explains the variation in ion species, we recommend that studies should be conducted during other seasons of the year and with more samples collected.

5 Appendix

Table A1. *Spearman's* correlation matrix of PM_1, anions, and cations at the Centro (CEN) and Tlaquepaque (TLA) sites

CEN													
	PM_1	$HCOO^-$	NO_3^-	SO_4^{2-}	$C_2O_4^{2-}$	∑Anions	Na^+	NH_4^+	K^+	Ca^{2+}	∑Cations	∑PSI	∑TI
PM_1	1.00												
$HCOO^-$	**0.80**	1.00											
NO_3^-	**0.65**	**0.88**	1.00										
SO_4^{2-}	**0.75**	**0.81**	**0.56**	1.00									
$C_2O_4^{2-}$	**0.76**	**0.96**	**0.88**	**0.80**	1.00								
∑Anions	**0.75**	**0.96**	**0.86**	**0.85**	**0.96**	1.00							
Na^+	**0.81**	**0.72**	**0.70**	**0.76**	**0.71**	**0.79**	1.00						
NH_4^+	**0.65**	**0.86**	**0.81**	**0.87**	**0.91**	**0.93**	**0.79**	1.00					
K^+	**0.79**	**0.79**	**0.75**	**0.69**	**0.84**	**0.76**	**0.72**	**0.74**	1.00				
Ca^{2+}	-0.27	-0.43	-0.44	-0.36	-0.51	**-0.57**	-0.38	-0.50	-0.15	1.00			
∑Cations	**0.82**	**0.87**	**0.80**	**0.85**	**0.90**	**0.88**	**0.85**	**0.88**	**0.92**	-0.23	1.00		
∑PSI	**0.68**	**0.90**	**0.82**	**0.88**	**0.92**	**0.97**	**0.79**	**0.98**	**0.71**	-0.55	0.87	1.00	
∑TI	**0.82**	**0.88**	**0.82**	**0.84**	**0.91**	**0.90**	**0.88**	**0.89**	**0.91**	-0.29	0.99	0.88	1.00
TLA													
	PM_1	$HCOO^-$	NO_3^-	SO_4^{2-}	$C_2O_4^{2-}$	∑Anions	Na^+	NH_4^+	K^+	Ca^{2+}	∑Cations	∑PSI	∑TI
PM_1	1.00												
$HCOO^-$	0.49	1.00											
NO_3^-	0.49	**0.70**	1.00										
SO_4^{2-}	0.28	**0.79**	**0.68**	1.00									
$C_2O_4^{2-}$	0.44	**0.67**	**0.68**	**0.90**	1.00								
∑Anions	0.33	**0.78**	**0.76**	**0.98**	**0.90**	1.00							
Na^+	0.38	**0.73**	0.39	**0.79**	**0.75**	**0.76**	1.00						
NH_4^+	0.28	**0.79**	**0.77**	**0.96**	**0.88**	**0.99**	**0.76**	1.00					
K^+	0.38	**0.78**	0.40	**0.80**	**0.81**	**0.73**	**0.89**	**0.73**	1.00				
Ca^{2+}	-0.16	0.11	0.06	0.12	0.07	0.16	0.09	0.17	0.15	1.00			
∑Cations	0.35	**0.81**	**0.70**	**0.93**	**0.86**	**0.95**	**0.86**	**0.96**	**0.79**	0.27	1.00		
∑PSI	0.30	**0.78**	**0.76**	**0.98**	**0.89**	**1.00**	**0.75**	**0.99**	**0.71**	0.12	**0.95**	1.00	
∑TI	0.35	**0.82**	**0.75**	**0.96**	**0.88**	**0.98**	**0.81**	**0.99**	**0.78**	0.20	**0.97**	**0.98**	1.00
Study Area													
	PM_1	$HCOO^-$	NO_3^-	SO_4^{2-}	$C_2O_4^{2-}$	∑Anions	Na^+	NH_4^+	K^+	Ca^{2+}	∑Cations	∑PSI	∑TI
PM_1	1.00												
$HCOO^-$	**0.63**	1.00											
NO_3^-	**0.55**	**0.79**	1.00										
SO_4^{2-}	**0.55**	**0.83**	**0.67**	1.00									
$C_2O_4^{2-}$	**0.61**	**0.83**	**0.78**	**0.91**	1.00								
∑Anions	**0.58**	**0.87**	**0.82**	**0.96**	**0.95**	1.00							
Na^+	**0.45**	**0.68**	**0.46**	**0.72**	**0.68**	**0.70**	1.00						
NH_4^+	**0.51**	**0.83**	**0.79**	**0.94**	**0.92**	**0.97**	**0.74**	1.00					
K^+	**0.54**	**0.80**	**0.57**	**0.77**	**0.82**	**0.76**	**0.78**	**0.75**	1.00				
Ca^{2+}	-0.20	-0.07	-0.15	-0.09	-0.15	-0.13	-0.13	-0.14	-0.00	1.00			
∑Cations	**0.53**	**0.83**	**0.74**	**0.91**	**0.88**	**0.92**	**0.82**	**0.93**	**0.83**	0.04	1.00		
∑PSI	**0.55**	**0.85**	**0.81**	**0.96**	**0.94**	**0.99**	**0.70**	**0.99**	**0.75**	-0.15	**0.92**	1.00	
∑TI	**0.54**	**0.87**	**0.79**	**0.93**	**0.92**	**0.95**	**0.79**	**0.96**	**0.85**	-0.01	**0.98**	**0.95**	1.00

∑Anions: sum anions; ∑Cations: sum cations; ∑PSI: sum principal secondary ions; ∑TI: sum total ions. Values with $p<0.5$ in bold

Table A2. *Spearman's* correlation matrix of *intrasite* and *intersite* meteorological parameters during the warm-dry period at the GMA

		CEN											TLA										
		AT	**MT**	**mT**	**HR**	**WS**	**MWS**	**AP**	**SR**	**MaxSR**	**UV**	**MaxUV**	**AT**	**MT**	**mT**	**HR**	**WS**	**MWS**	**AP**	**SR**	**MaxSR**	**UV**	**MaxUV**
CEN	**AT**	1.00																					
	MT	**1.00**	1.00																				
	mT	**1.00**	**1.00**	1.00																			
	HR	-0.46	-0.46	-0.46	1.00																		
	WS	-0.14	-0.14	-0.14	0.00	1.00																	
	MWS	0.08	0.08	0.08	-0.09	**0.82**	1.00																
	AP	-0.42	-0.42	-0.42	-0.04	0.12	0.08	1.00															
	SR	0.44	0.44	0.44	**-0.73**	-0.09	-0.11	0.38	1.00														
	MaxSR	-0.35	-0.35	-0.35	-0.08	0.02	-0.30	-0.15	-0.04	1.00													
	UV	**0.60**	**0.60**	**0.60**	**-0.81**	0.09	0.03	0.08	**0.87**	0.11	1.00												
	MaxUV	0.31	0.31	0.31	**-0.63**	-0.09	-0.28	-0.15	**0.59**	**0.59**	**0.79**	1.00											
TLA	**AT**	**0.93**											1.00										
	MT	**0.93**	**0.93**										**1.00**	1.00									
	mT	**0.93**	**0.93**	**0.93**									**1.00**	**1.00**	1.00								
	HR	-0.18	-0.18	-0.18	**0.81**								-0.30	-0.34	-0.30	1.00							
	WS	-0.14	-0.14	-0.14	0.42	0.21							0.04	0.06	0.04	0.16	1.00						
	MWS	-0.19	-0.19	-0.19	0.34	0.40	0.44						-0.02	-0.01	-0.02	0.14	**0.91**	1.00					
	AP	-0.46	-0.46	-0.46	-0.01	0.30	0.20	**0.93**					-0.47	-0.46	-0.47	0.11	0.05	-0.07	1.00				
	SR	**0.54**	**0.54**	**0.54**	**-0.76**	-0.26	-0.27	0.06	**0.85**				**0.54**	**0.56**	**0.54**	**-0.62**	-0.37	-0.48	0.12	1.00			
	MaxSR	-0.14	-0.14	-0.14	-0.07	-0.22	-0.52	-0.07	0.21	**0.83**			-0.12	-0.12	-0.12	-0.38	-0.42	-0.48	-0.22	0.06	1.00		
	UV	0.48	0.48	0.48	**-0.80**	-0.14	-0.24	0.04	**0.85**	0.24	**0.89**		0.46	0.49	0.46	**-0.69**	**-0.57**	**-0.63**	0.07	**0.92**	0.33	1.00	
	MaxUV	-0.11	-0.11	-0.01	-0.42	-0.13	-0.43	0.04	0.42	**0.78**	**0.54**	**0.82**	-0.14	-0.12	-0.14	**-0.60**	**-0.65**	**-0.63**	-0.06	0.32	**0.81**	**0.58**	1.00

AT: average temperature (24 h); MT: maximum temperature; mT: minimum temperature; RH: relative humidity; WS: wind speed; MWS: maximum wind speed; AP: atmospheric pressure; SR: solar radiation; MaxSR: maximum solar radiation; UV: ultraviolet radiation; MaxUV: maximum ultraviolet radiation. Values with $p<0.5$ in bold.

Table A3. *Spearman's* correlation matrix of the PM_1, anions, cations, and meteorological parameters by site and study area

		PM_1	**$HCOO^-$**	**NO_3^-**	**SO_4^{2-}**	**$C_2O_4^{2-}$**	**Na^+**	**NH_4^+**	**K^+**	**Ca^{2+}**	**∑Ani**	**∑Cat**	**∑PSI**
CEN	AT	0.51	0.19	-0.11	**0.56**	0.14	0.36	0.25	0.15	-0.03	0.21	0.27	0.27
	MT	0.51	0.19	-0.11	**0.56**	0.14	0.36	0.25	0.15	-0.03	0.21	0.27	0.27
	mT	0.51	0.19	-0.11	**0.56**	0.14	0.36	0.25	0.15	-0.03	0.21	0.27	0.27
	RH	0.23	0.53	**0.59**	0.34	**0.57**	0.25	0.47	**0.59**	-0.03	0.50	**0.59**	0.48
	WS	-0.10	0.01	0.02	0.09	0.07	-0.04	0.10	0.03	-0.15	0.06	0.07	0.10
	MWS	0.31	0.32	0.18	0.28	0.32	0.10	0.22	0.17	-0.23	0.29	0.24	0.27
	AP	0.05	-0.05	0.18	-0.29	-0.07	0.04	-0.17	0.17	-0.07	-0.10	-0.12	-0.21
	SR	-0.13	-0.38	-0.44	-0.16	-0.38	-0.17	-0.31	-0.22	-0.07	-0.33	-0.41	-0.33
	MaxSR	**-0.91**	**-0.78**	**-0.63**	**-0.69**	**-0.81**	**-0.68**	**-0.63**	**-0.81**	0.41	**-0.73**	**-0.76**	**-0.64**
	UV	-0.19	**-0.58**	**-0.68**	-0.20	**-0.57**	-0.25	-0.45	-0.41	0.08	-0.52	-0.49	-0.47
	MaxUV	**-0.63**	**-0.89**	**-0.94**	-0.55	**-0.88**	**-0.63**	**-0.74**	**-0.76**	0.35	**-0.84**	**-0.80**	**-0.76**
		PM_1	**$HCOO^-$**	**NO_3^-**	**SO_4^{2-}**	**$C_2O_4^{2-}$**	**Na^+**	**NH_4^+**	**K^+**	**Ca^{2+}**	**∑Ani**	**∑Cat**	**∑PSI**
TLA	AT	0.27	0.31	-0.15	0.40	0.31	0.47	0.25	0.40	0.01	0.32	0.36	0.31
	MT	0.23	0.25	-0.20	0.37	0.30	0.47	0.21	0.38	0.03	0.29	0.34	0.28
	mT	0.27	0.31	-0.15	0.40	0.31	0.47	0.25	0.40	0.01	0.32	0.36	0.31
	RH	0.12	**0.65**	**0.68**	**0.66**	0.48	0.34	**0.66**	0.46	0.28	**0.65**	**0.60**	**0.63**
	WS	0.52	0.30	**0.67**	0.45	**0.71**	0.36	0.55	0.33	0.16	**0.57**	0.50	**0.57**
	MWS	0.51	0.26	**0.69**	0.43	**0.70**	0.34	0.52	0.36	0.14	0.55	0.47	0.53
	AP	0.01	-0.30	0.05	-0.15	-0.04	-0.29	-0.08	-0.23	-0.29	-0.13	-0.21	-0.10
	SR	-0.16	-0.25	**-0.64**	-0.15	-0.18	0.10	-0.23	-0.05	-0.44	-0.24	-0.16	-0.19
	MaxSR	-0.15	-0.25	-0.39	**-0.65**	**-0.72**	-0.33	**-0.59**	-0.48	0.05	**-0.61**	-0.54	-0.62
	UV	-0.26	-0.45	**-0.80**	-0.36	-0.45	-0.10	-0.45	-0.28	-0.34	-0.44	-0.37	-0.41
	MaxUV	-0.24	-0.52	**-0.69**	**-0.86**	**-0.90**	-0.49	**-0.85**	**-0.62**	-0.16	**-0.86**	**-0.74**	**-0.87**
		PM_1	**$HCOO^-$**	**NO_3^-**	**SO_4^{2-}**	**$C_2O_4^{2-}$**	**Na^+**	**NH_4^+**	**K^+**	**Ca^{2+}**	**∑Ani**	**∑Cat**	**∑PSI**
Study Area	AT	**0.39**	0.22	-0.13	**0.46**	0.23	**0.42**	0.27	0.24	-0.01	0.28	0.33	0.29
	MT	0.38	0.20	-0.14	**0.45**	0.23	**0.41**	0.26	0.24	0.00	0.27	0.33	0.28
	mT	**0.39**	0.22	-0.13	**0.46**	0.23	**0.42**	0.27	0.24	-0.01	0.28	0.33	0.29
	RH	0.17	**0.62**	**0.64**	**0.51**	**0.56**	0.26	**0.56**	**0.52**	0.19	**0.58**	**0.56**	**0.57**
	WS	0.20	0.20	0.33	0.30	0.37	0.21	0.32	0.18	0.00	0.33	0.28	0.33
	MWS	**0.39**	0.29	**0.40**	0.39	**0.46**	0.25	0.36	0.25	-0.06	**0.42**	0.35	**0.39**
	AP	0.27	0.06	0.13	-0.02	0.07	-0.23	-0.04	0.02	-0.02	0.04	-0.13	0.00
	SR	-0.13	-0.34	**-0.56**	-0.19	-0.31	0.03	-0.28	-0.14	-0.32	-0.31	-0.28	-0.29
	MaxSR	**-0.56**	**-0.50**	**-0.50**	**-0.68**	**-0.74**	**-0.49**	**-0.64**	**-0.65**	0.21	**-0.68**	**-0.66**	**-0.66**
	UV	0.00	-0.35	**-0.60**	-0.22	**-0.39**	-0.26	**-0.40**	-0.29	-0.01	-0.37	**-0.39**	-0.38
	MaxUV	0.05	-0.36	**-0.48**	**-0.42**	**-0.51**	**-0.48**	**-0.52**	**-0.42**	0.15	**-0.50**	**-0.52**	**-0.50**

AT: average temperature (24 h); MT: maximum temperature; mT: minimum temperature; RH: relative humidity; WS: wind speed; WD: wind direction; MWS: maximum wind speed; AP: atmospheric pressure; SR: solar radiation; MaxSR: maximum solar radiation; UV: ultraviolet radiation; MaxUV: maximum ultraviolet radiation; ∑PSI: sum major secondary ions; ∑TI: sum total ions. Values with $p<0.5$ in bold.

6 References

Agudelo-Castañeda, D. M., & Teixeira, E. C. (2014). Seasonal changes, identification and source apportionment of PAH in PM1.0. *Atmospheric Environment*, *96*(OCTOBER), 186–200. https://doi.org/10.1016/j.atmosenv.2014.07.030

Aldabe, J., Elustondo, D., Santamaría, C., Lasheras, E., Pandolfi, M., Alastuey, A., Querol, X., & Santamaría, J. M. (2011). *Chemical characterisation and source apportionment of PM2.5 and PM10 at rural, urban and traffic sites in Navarra (North of Spain)*. https://doi.org/10.1016/j.atmosres.2011.07.003

Cheng, Y., Zou, S. C., Lee, S. C., Chow, J. C., Ho, K. F., Watson, J. G., Han, Y. M., Zhang, R. J., Zhang, F., Yau, P. S., Huang, Y., Bai, Y., & Wu, W. J. (2011). Characteristics and source apportionment of PM 1 emissions at a roadside station. *Journal of Hazardous Materials*, *195*, 82–91. https://doi.org/10.1016/j.jhazmat.2011.08.005

Chung, A., Herner, J. D., & Kleeman, M. J. (2001). Detection of alkaline ultrafine atmospheric particles at Bakersfield, California. *Environmental Science & Technology*, *35*(11), 2184–2190.

Díaz-Torres, J. J., Hernández-Mena, L., Murillo-Tovar, M. A., León-Becerril, E., López-López, A., Suárez-Plascencia, C., Aviña-Rodriguez, E., Barradas-Gimate, A., & Ojeda-Castillo, V. (2017). Assessment of the modulation effect of rainfall on solar radiation availability at the Earth's surface. *Meteorological Applications*, *24*(2), 180–190. https://doi.org/10.1002/met.1616

Du, H., Kong, L., Cheng, T., Chen, J., Du, J., Li, L., Xia, X., Leng, C., & Huang, G. (2011). Insights into summertime haze pollution events over Shanghai based on online water-soluble ionic composition of aerosols. *Atmospheric Environment*, *45*(29), 5131–5137. https://doi.org/10.1016/j.atmosenv.2011.06.027

Engling, G., Zhang, Y. N., Chan, C. Y., Sang, X. F., Lin, M., Ho, K. F., Li, Y. S., Lin, C. Y., & Lee, J. J. (2011). Characterization and sources of aerosol particles over the southeastern Tibetan Plateau during the Southeast Asia biomass-burning season. *Tellus, Series B: Chemical and Physical Meteorology*, *63*(1), 117–128. https://doi.org/10.1111/j.1600-0889.2010.00512.x

Feng, J. L., Guo, Z. G., Zhang, T. R., Yao, X. H., Chan, C. K., & Fang, M. (2012). Source and formation of secondary particulate matter in PM<inf>2.5</inf> in Asian continental outflow. *Journal of Geophysical Research Atmospheres*, *117*(3), 1–11. https://doi.org/10.1029/2011JD016400

Finlayson-Pitts, B. J., & Pitts, J. J. N. (2000). *Chemistry of the Upper and Lower Atmosphere. Theory, Experiments, and Applications*. Academic Press.

Finlayson-Pitts, Barbara J., & Pitts, J. J. N. (2000). *Chemistry of the Upper and Lower Atmosphere. Theory, Experiments, and Applications*. Academic Press.

Gaffney, J. S., & Marley, N. A. (2009). The impacts of combustion emissions on air quality and climate – From coal to biofuels and beyond. *Atmospheric Environment*, *43*, 23–36. https://doi.org/10.1016/j.atmosenv.2008.09.016

Glasius, M., Wessel, S., Christensen, C. S., Jacobsen, J. K., Jorgensen, H. E., Klitgaard, K. C., Petersen, L., Rasmussen, J. K., Hansen, T. S., Lohse, C., Boaretto, E., & Heinemeier, J. (2000). Sources to formic acid studied by carbon isotopic analysis and air mass characterization. *Atmospheric Environment*, *34*, 2471–2479.

Gomišček, B., Hauck, H., Stopper, S., & Preining, O. (2004). Spatial and temporal variations of PM1, PM2.5, PM10 and particle number concentration during the AUPHEP - Project. *Atmospheric Environment*, *38*, 3917–3934. https://doi.org/10.1016/j.atmosenv.2004.03.056

Guo, S., Hu, M., Wang, Z. B., Slanina, J., & Zhao, Y. L. (2010). Size-resolved aerosol water-soluble ionic compositions in the summer of Beijing: implication of regional secondary formation. *Atmospheric Chemistry and Physics*, *10*, 947–959.

Guzmán-Torres, D., Eiguren-Fernández, A., Cicero-Fernández, P., Maubert-Franco, M., Retama-Hernández, A., Ramos Villegas, R., & Miguel, A. H. (2009). Effects of meteorology on diurnal and nocturnal levels of priority polycyclic aromatic hydrocarbons and elemental and organic carbon in PM10 at a source and a receptor area in Mexico City. *Atmospheric Environment*, *43*, 2693–2699. https://doi.org/10.1016/j.atmosenv.2009.03.003

Harrison, R. M., Jones, A. M., & Lawrence, R. G. (2004). Major component composition of PM 10 and PM 2.5 from roadside and urban background sites. *Atmospheric Environment*, *38*, 4531–4538. https://doi.org/10.1016/j.atmosenv.2004.05.022

Harrison, R. M., & Yin, J. (2000). Particulate matter in the atmosphere: which particle properties are important for its effects on health? *The Science of the Total Environment*, *249*, 85–101.

Hernandez-Mena, L., Gallardo Valdez, J., Díaz-Torres, J. de J., & Villegas García, E. (2017). Contaminación del aire por partículas (PM10) en el Polígono de Fragilidad Ambiental, Guadalajara, Jalisco. *Reaxion, Ciencia y Tecnología Universitaria*, *2*(4), 12–25.

Herrmann, P., & Hänel, G. (1997). Wintertime optical properties of atmospheric particles and weather. *Atmospheric Environment*, *31*(24), 4053–4062.

Hsieh, L.-Y., Chen, C.-L., Wan, M.-W., Tsai, C.-H., & Tsai, Y. I. (2008). Speciation and temporal characterization of dicarboxylic acids in PM 2.5 during a PM episode and a period of non-episodic pollution. *Atmospheric Environment*, *42*, 6836–6850. https://doi.org/10.1016/j.atmosenv.2008.05.021

Hsieh, L.-Y., Kuo, S.-C., Chen, C.-L., & Tsai, Y. I. (2009). Size distributions of nano/micron dicarboxylic acids and inorganic ions in suburban PM episode and non-episodic aerosol. *Atmospheric Environment*, *43*, 4396–4406. https://doi.org/10.1016/j.atmosenv.2009.04.034

Huang, X. F., Xue, L., Tian, X. D., Shao, W. W., Sun, T. Le, Gong, Z. H., Ju, W. W., Jiang, B., Hu, M., & He, L. Y. (2013). Highly time-resolved carbonaceous aerosol characterization in Yangtze River Delta of China: Composition, mixing state and secondary formation. *Atmospheric Environment*, *64*, 200–207. https://doi.org/10.1016/j.atmosenv.2012.09.059

Huang, X., Liu, Z., Zhang, J., Wen, T., Ji, D., & Wang, Y. (2016). Seasonal variation and secondary formation of size-segregated aerosol water-soluble inorganic ions during pollution episodes in Beijing. *Atmospheric Research*, *168*, 70–79. https://doi.org/10.1016/j.atmosres.2015.08.021

Instituto Nacional de Estadística y Geografía (INEGI). (2010). *Instituto Nacional de Estadística y Geografía (INEGI)*. http://www.inegi.org.mx/

Jacobson, M. C., Hansson, H.-C., Noone, K. J., & Charlson, R. J. (2000). Organic atmospheric aerosols: Review and state of the science. *Reviews of Geophysics*, *38*(2), 267–294. https://doi.org/10.1029/1998RG000045

Kawamuras, K., & Kaplan, I. R. (1987). Motor Exhaust Emissions as a Primary Source for Dicarboxylic Acids in Los Angeles Ambient Air. *Enviromental Science & Tecnology*, *21*(20), 105–110.

Koçak, M., Mihalopoulos, N., & Kubilay, N. (2007). Chemical composition of the fine and coarse fraction of aerosols in the northeastern Mediterranean. *Atmospheric Environment*, *41*, 7351–7368. https://doi.org/10.1016/j.atmosenv.2007.05.011

Langner, J., & Rodhe, H. (1991). A Global Three-Dimensional Model of the Tropospheric Sulfur Cycle. *Journal of Atmospheric Chemistry*, *13*(22), 5–263.

Laongsri, B., & Harrison, R. M. (2013). Atmospheric behaviour of particulate oxalate at UK urban background and rural sites. *Atmospheric Environment*, *71*, 319–326. https://doi.org/10.1016/j.atmosenv.2013.02.015

Lee, C.-T., Chuang, M.-T., Lin, N.-H., Wang, J.-L., Sheu, G.-R., Chang, S.-C., Wang, S.-H., Huang, H., Chen, H.-W., Liu, Y.-L., Weng, G.-H., Lai, H.-Y., & Hsu, S.-P. (2011). The enhancement of PM 2.5 mass and water-soluble ions of biosmoke transported from Southeast Asia over the Mountain Lulin site in Taiwan. *Atmospheric Environment*, *45*, 5784–5794. https://doi.org/10.1016/j.atmosenv.2011.07.020

Legrand, M., Preunkert, S., Oliveira, T., Pio, C. A., Hammer, S., Gelencsér, A., Kasper-Giebl, A., & Laj, P. (2007). Origin of C2-C5 dicarboxylic acids in the European atmosphere inferred from year-round aerosol study conducted at a west-east transect. *Journal of Geophysical Research Atmospheres*, *112*(23), 1–14. https://doi.org/10.1029/2006JD008019

Li, H. J., Zhu, T., Zhao, D. F., Zhang, Z. F., & Chen, Z. M. (2010). Kinetics and mechanisms of heterogeneous reaction of NO2 on CaCO3 surfaces under dry and wet conditions. *Atmospheric Chemistry and Physics*, *10*, 463–474.

Lim, H.-J., Carlton, A. G., & Turpin, B. J. (2005). Isoprene Forms Secondary Organic Aerosol through Cloud Processing: Model Simulations. *Environmental Science & Technology*, *39*, 4441–4446. https://doi.org/10.1021/es048039h

Marley, N. A., Gaffney, J. S., Baird, J. C., Blazer, C. A., Drayton, P. J., & Frederick, J. E. (2001). An Empirical Method for the Determination of the Complex Refractive Index of Size-Fractionated Atmospheric Aerosols for Radiative Transfer Calculations. *Aerosol Science and Technology*, *34:6*, 535–549. https://doi.org/10.1080/02786820118599

Massey, D., Kulshrestha, A., Masih, J., & Taneja, A. (2012). Seasonal trends of PM10, PM5.0, PM2.5 & PM1.0 in indoor and outdoor environments of residential homes located in North-Central India. *Building and Environment*, *47*(1), 223–231. https://doi.org/10.1016/j.buildenv.2011.07.018

Minguillón, M. C., Querol, X., Baltensperger, U., & Prévôt, A. S. H. (2012). *Fine and coarse PM composition and sources in rural and urban sites in Switzerland: Local or regional pollution?* https://doi.org/10.1016/j.scitotenv.2012.04.030

Moya, M., Castro, T., Zepeda, M., & Baez, A. (2003). Characterization of size-differentiated inorganic composition of aerosols in Mexico City. *Atmospheric Environment*, *37*, 3581–3591. https://doi.org/10.1016/S1352-2310(03)00345-5

Pateraki, S., Asimakopoulos, D. N., Bougiatioti, a., Maggos, T., Vasilakos, C., & Mihalopoulos, N. (2014). Assessment of PM2.5 and PM1 chemical profile in a multiple-impacted Mediterranean urban area: Origin, sources and meteorological dependence. *Science of the Total Environment*, *479–480*, 210–220. https://doi.org/10.1016/j.scitotenv.2014.02.008

Perrone, M. R., Becagli, S., Garcia Orza, J. a., Vecchi, R., Dinoi, a., Udisti, R., & Cabello, M. (2013). The impact of long-range-transport on PM1 and PM2.5 at a Central Mediterranean site. *Atmospheric Environment*, *71*(2013), 176–186. https://doi.org/10.1016/j.atmosenv.2013.02.006

Querol, X., Alastuey, A., Lopez-Soler, A., Plana, F., Puicercus, J. A., Mantilla, E., & Palau, J. L. (1999). Daily evolution of sulphate aerosols in a rural area, northeastern Spain-elucidation of an atmospheric reservoir effect. *Environmental Pollution*, *105*, 397–407.

Seinfeld, J. H., & Pandis, S. N. (2006). *Atmospheric chemistry and physics : from air pollution to climate change*. J. Wiley.

Squizzato, S., Masiol, M., Agostini, C., Visin, F., Formenton, G., Harrison, R. M., & Rampazzo, G. (2016). *Factors, origin and sources affecting PM 1 concentrations and composition at an urban background site*. https://doi.org/10.1016/j.atmosres.2016.06.002

Titos, G., Lyamani, H., Pandolfi, M., Alastuey, A., & Alados-Arboledas, L. (2014). Identification of fine (PM 1) and coarse (PM 10-1) sources of particulate matter in an urban environment. *Atmospheric Environment*, *89*, 593–602. https://doi.org/10.1016/j.atmosenv.2014.03.001

Tsai, J.-H., Lin, J.-H., Yao, Y.-C., & Chiang, H.-L. (2012). Size distribution and water soluble ions of ambient particulate matter on episode and non-episode days in southern Taiwan. *Aerosol and Air Quality Research*, *12*(2), 263–274. https://doi.org/10.4209/aaqr.2011.10.0167

Tsai, Y. I., & Chen, C.-L. (2006). Atmospheric aerosol composition and source apportionments to aerosol in southern Taiwan. *Atmospheric Environment*, *40*, 4751–4763. https://doi.org/10.1016/j.atmosenv.2006.04.029

Tsai, Y. I., Hsieh, L.-Y., Weng, T.-H., Ma, Y.-C., & Kuo, S.-C. (2008). *A novel method for determination of low molecular weight dicarboxylic acids in background atmospheric aerosol using ion chromatography*. https://doi.org/10.1016/j.aca.2008.07.041

Tsai, Y. I., Sopajaree, K., Chotruksa, A., Wu, H.-C., & Kuo, S.-C. (2013). Source indicators of biomass burning associated with inorganic salts and carboxylates in dry season ambient aerosol in Chiang Mai Basin, Thailand. *Atmospheric Environment*, *78*, 93–104. https://doi.org/10.1016/j.atmosenv.2012.09.040

Tsai, Y. I., Wu, P.-L., Hsu, Y.-T., & Yang, C.-R. (2010). *Anhydrosugar and sugar alcohol organic markers associated with carboxylic acids in particulate matter from incense burning*. https://doi.org/10.1016/j.atmosenv.2010.06.030

Turšič, J., Berner, A., Podkrajšek, B., & Grgić, I. (2004). Influence of ammonia on sulfate formation under haze conditions. *Atmospheric Environment*, *38*, 2789–2795. https://doi.org/10.1016/j.atmosenv.2004.02.036

Wang, G. H., Zhou, B. H., Cheng, C. L., Cao, J. J., Li, J. J., Meng, J. J., Tao, J., Zhang, R. J., & Fu, P. Q. (2013). Impact of Gobi desert dust on aerosol chemistry of Xi'an, inland China during spring 2009: differences in composition and size distribution between the urban ground surface and the mountain atmosphere. *Atmos. Chem. Phys. Atmospheric Chemistry and Physics*, *13*, 819–835. https://doi.org/10.5194/acp-13-819-2013

Wang, Y., Zhuang, G., Chen, S., An, Z., & Zheng, A. (2007). Characteristics and sources of formic, acetic and oxalic acids in PM 2.5 and PM 10 aerosols in Beijing, China. *Atmospheric Research*, *84*, 169–181. https://doi.org/10.1016/j.atmosres.2006.07.001

Wang, Y., Zhuang, G., Sun, Y., & An, Z. (2006). The variation of characteristics and formation mechanisms of aerosols in dust, haze, and clear days in Beijing. *Atmospheric Environment*, *40*, 6579–6591. https://doi.org/10.1016/j.atmosenv.2006.05.066

Wenger, D., Gerecke, A. C., Heeb, N. V., Hueglin, C., Seiler, C., Haag, R., Naegeli, H., & Zenobi, R. (2009). Aryl hydrocarbon receptor-mediated activity of atmospheric particulate matter from an urban and a rural site in Switzerland. *Atmospheric Environment*, *43*(22–23), 3556–3562. https://doi.org/10.1016/j.atmosenv.2009.04.012

Whitby, K. T. (1978). The physical characteristics of sulfur aerosol. *Atmospheric Environment*, *12*, 135–159.

Yan, J., Chen, L., Lin, Q., Li, Z., Chen, H., & Zhao, S. (2015). Chemical characteristics of submicron aerosol particles during a long- lasting haze episode in Xiamen, China. *Atmospheric Environment*, *113*, 118–126. https://doi.org/10.1016/j.atmosenv.2015.05.003

Yang, F., Gu, Z., Feng, J., Liu, X., & Yao, X. (2014). Biogenic and anthropogenic sources of oxalate in PM 2.5 in a mega city, Shanghai. *Atmospheric Research*, *138*, 356–363. https://doi.org/10.1016/j.atmosres.2013.12.006

Zhang, Y. W., Zhang, X. Y., Zhang, Y. M., Shen, X. J., Sun, J. Y., Ma, Q. L., Yu, X. M., Zhu, J. L., Zhang, L., & Che, H. C. (2015). Significant concentration changes of chemical components of PM 1 in the Yangtze River Delta area of China and the implications for the formation mechanism of heavy haze–fog pollution. *Science of the Total Environment*, *538*, 7–15. https://doi.org/10.1016/j.scitotenv.2015.06.104